

Desert Environment and Climate Observation Network over the Taklimakan Desert

Fan Yang, Qing He, Jianping Huang, Ali Mamtimin, Xinghua Yang, Wen Huo, Chenglong Zhou, Xinchun Liu, Wenshou Wei, Caixia Cui, Minzhong Wang, Hongjun Li, Lianmei Yang, Hongsheng Zhang, Yuzhi Liu, Xinqian Zheng, Honglin Pan, Lili Jin, Han Zou, Libo Zhou, Yongqiang Liu, Jiantao Zhang, Lu Meng, Yu Wang, Xiaolin Qin, Yongjun Yao, Houyong Liu, Fumin Xue, and Wei Zheng

ABSTRACT: As the second-largest shifting sand desert worldwide, the Taklimakan Desert (TD) represents the typical aeolian landforms in arid regions as an important source of global dust aerosols. It directly affects the ecological environment and human health across East Asia. Thus, establishing a comprehensive environment and climate observation network for field research in the TD region is essential to improve our understanding of the desert meteorology and environment, assess its impact, mitigate potential environmental issues, and promote sustainable development. With a nearly 20-yr effort under the extremely harsh conditions of the TD, the Desert Environment and Climate Observation Network (DECON) has been established completely covering the TD region. The core of DECON is the Tazhong station in the hinterland of the TD. Moreover, the network also includes 4 satellite stations located along the edge of the TD for synergistic observations, and 18 automatic weather stations interspersed between them. Thus, DECON marks a new chapter of environmental and meteorological observation capabilities over the TD, including dust storms, dust emission and transport mechanisms, desert land–atmosphere interactions, desert boundary layer structure, ground calibration for remote sensing monitoring, and desert carbon sinks. In addition, DECON promotes cooperation and communication within the research community in the field of desert environments and climate, which promotes a better understanding of the status and role of desert ecosystems. Finally, DECON is expected to provide the basic support necessary for coordinated environmental and meteorological monitoring and mitigation, joint construction of ecologically friendly communities, and sustainable development of central Asia.

Keywords: Atmosphere-land interaction; Automatic weather stations; Boundary Layer; Desert Meteorology; Dust or dust storms; Surface observations

<https://doi.org/10.1175/BAMS-D-20-0236.1>

Corresponding author: Jianping Huang, hjp@lzu.edu.cn

In final form 15 January 2021

©2021 American Meteorological Society

For information regarding reuse of this content and general copyright information, consult the [AMS Copyright Policy](#).

AFFILIATIONS: F. Yang, He, Ali, X. Yang, Huo, C. Zhou, X. Liu, Wei, Cui, M. Wang, Li, L. Yang, X. Zheng, Pan, Jin, Yo. Liu, J. Zhang, Meng, and Y. Wang—Institute of Desert Meteorology/Taklimakan Desert Meteorology Field Experiment Station, China Meteorological Administration, Urumqi, China; **Huang and Yu. Liu**—Collaborative Innovation Center for Western Ecological Safety, Lanzhou University, Lanzhou, China; **H. Zhang**—Department of Atmospheric Science, School of Physics, Peking University, Beijing, China; **Zou and L. Zhou**—Institute of Atmospheric Physics, Chinese Academy of Sciences, Beijing, China; **Qin and Yao**—Beijing Truvel Instruments, Inc., Beijing, China; **H. Liu, Xue, and W. Zheng**—Tazhong Meteorological Bureau, Qiemo, China

The Tibetan Plateau (TP) strengthens the Asian monsoon circulation on the one hand, but on the other hand it blocks the transportation of warm and humid air from the Indian Ocean to inner Asia, and a downdraft forms on the northern side of the plateau, which contributes to the aridification of inland areas of Asia (Ye and Gao 1979; Manabe and Broccoli 1990; Liu et al. 2001; Ma et al. 2017). At the same time, it also accelerates the formation of the Taklimakan Desert (TD). The TD is the world's second-largest shifting sand desert with an area of 3.376×10^5 km², located in the Tarim basin (TB) of northwest China, which is the hinterland of Eurasia. It has the characteristics of being located far from the sea and exhibiting the driest climate, the rarest vegetation, the most complex dune types, the highest mobility of dunes, the largest proportion of shifting sand areas, the thickest shifting sand layer, and the smallest sand particle size. Its natural features are unique and typical among deserts around the world and aeolian landforms in arid areas (Yang et al. 2020a). Furthermore, sand and dust weather is common there (Wang et al. 2005; Huang et al. 2018). Annually, dust storms last longer than 10 days on average, and the longest dust storm lasted approximately 47 days; annual blowing sand weather conditions last more than 30 days on average, with the longest duration at 86 days; suspended dust weather conditions last for 20–200 days a year, which is common in the south of the TD. And the longest suspended dust weather lasted for 260 days in the south of the TD (Yang et al. 2016a). Compared to other deserts in the world, the dust aerosols over the TD exhibit a more notable absorptivity (Huang et al. 2014). In addition, the basin topography, particularly the effects of the TP on the regional meteorological field, coupled with the notable surface heating and convection and extreme turbulence of the desert surface in summer (Zhang and Wang 2008; Xu et al. 2014), contribute to frequent seasonal local dust storms (Han et al. 2005). In addition, these conditions facilitate the development of a hyperelevated atmospheric boundary layer at a height ranging from 3 to 5 km, as well as strong heating effects due to the dust aerosols stagnating at heights from 3 to 5 km in the troposphere in summer in the basin (Meng et al. 2019). The large amount of dust aerosols in this region affects the local environment and human health, and these aerosols are also transported by high-altitude westerlies to the lower reaches via uplift by the convergence current with the TP topography. This greatly impacts cloud cover and precipitation, surface energy distribution, ice and snow melting in East Asia and even globally, and ecosystem material cycles (Huang et al. 2007, 2008; Eguchi et al. 2009; Shao et al. 2011; Ge et al. 2014; Chen et al. 2014; Huang et al. 2018; Liu et al. 2020a; Filonchyk et al. 2020). It is estimated that the annual emission of dust aerosols in the TD amounts to approximately 187.31 Tg a⁻¹, accounting for approximately 31.0% of that in East Asia, which is an important source area of global dust aerosols (Gong et al. 2003; Zhang et al. 2003; Liu 2016; Chen et al. 2017a,b).

The oasis area surrounding the TD occupies 53.5% of the oasis in Xinjiang, feeding 11.34 million residents, accounting for up to 48% of the total population of Xinjiang (Xinjiang Bureau of Statistics 2017). There are abundant oil and gas resources under the vast desert, which has become one of the main regions producing oil and gas in China. The abundant groundwater reserves here total approximately 11–14.8 billion cubic meters, which is

10 times the capacity of the five Great Lakes in North America. Consequently, this area provides a key resource for northwest China to cope with drought and desertification and to maintain an ecological balance for a sustainable future. Historically, as a paramount corridor of the southern portion of the ancient Silk Road, the human activities around the TD have always been notable (Han et al. 2014), and it has an important bearing on the modern economy and culture of central Asia (Yang 2019).

Based on the aforementioned considerations, it is necessary to establish a comprehensive meteorological and environmental observation network over the TD. This observation network could support comprehensive field observation research of the desert meteorology, including studies related to dust storms and their widespread effects, dust emission and transportation, desert land–atmosphere interactions, desert boundary layer structure, remote sensing monitoring, and desert carbon sink in desert areas. More importantly, the establishment of such a network in the TD could enhance the required environmental and meteorological support capabilities serving the scientific and technological needs faced in balancing the development of the social economy and culture in central Asia with sustainable practices. Hence, the Institute of Desert Meteorology (IDM), China Meteorological Administration (CMA) has established the Desert Environment and Climate Observation Network (DECON) covering the TD. A long-awaited construction project, the completion of DECON, has initiated comprehensive research collaborations as a first-class domestic and international scientific experimental and training base, with state-of-the-art facilities, hardware, and software for various large-scale projects and research tasks.

An overview of the observation network

Design principle and composition. DECON is mainly composed of five observation stations (please refer to Fig. 1), including the Tazhong, Xiaotang, Minfeng, Hongliuhe, and Khunjerab stations. The Tazhong station, at the core of the monitoring station network, is the only desert environment and climate station worldwide that penetrates the hinterland of a shifting desert by more than 200 km. The Tazhong station, the first DECON station established in 2002, is located at the center of the TD and is equipped with the most comprehensive observation equipment for experimental studies. The other four satellite stations (the Xiaotang, Minfeng, Hongliuhe, and Khunjerab stations) were established to perform synergistic observations and research with the Tazhong station. Among them, the Xiaotang station, located approximately 220 km north of the center of the TD in the oasis-desert ecotone of Xiaotang, was completely equipped in 2015. Subsequently, the Hongliuhe and Khunjerab stations, located 400 km east and 200 km west, respectively, of the TD, were established in 2016. Both of these sites are critical for the monitoring and evaluation of dust transport and its impact, owing to their east/west locations. In 2018, the Minfeng station was established in the Yeyike Township of Minfeng County, located along the southern margin of the TD and north Kunlun Mountains. Due to the Minfeng station location on the northern slope of the TP, this station may provide a key understanding of the interaction between the TD and TP, especially in regard to the influence of the thermal differences between the desert and plateau on dust-storm development in the TD, as well as the long-distance transport of dust influenced by the plateau topography. In addition, to compensate for the gaps between the stations and to continuously capture meteorological dust-storm data, 18 automatic weather stations were constructed across the TD in 2010, providing wind speed, wind direction, air temperature, air humidity, air pressure, and precipitation data.

Overall, the configuration of DECON, centered on the Tazhong station, combining 4 satellite stations and 18 automatic weather stations, provides a good coverage of the TD for environmental and climatic studies. Based on the observation experiments conducted in DECON for nearly 20 years, the experimental results show a high representativeness and reference value regarding

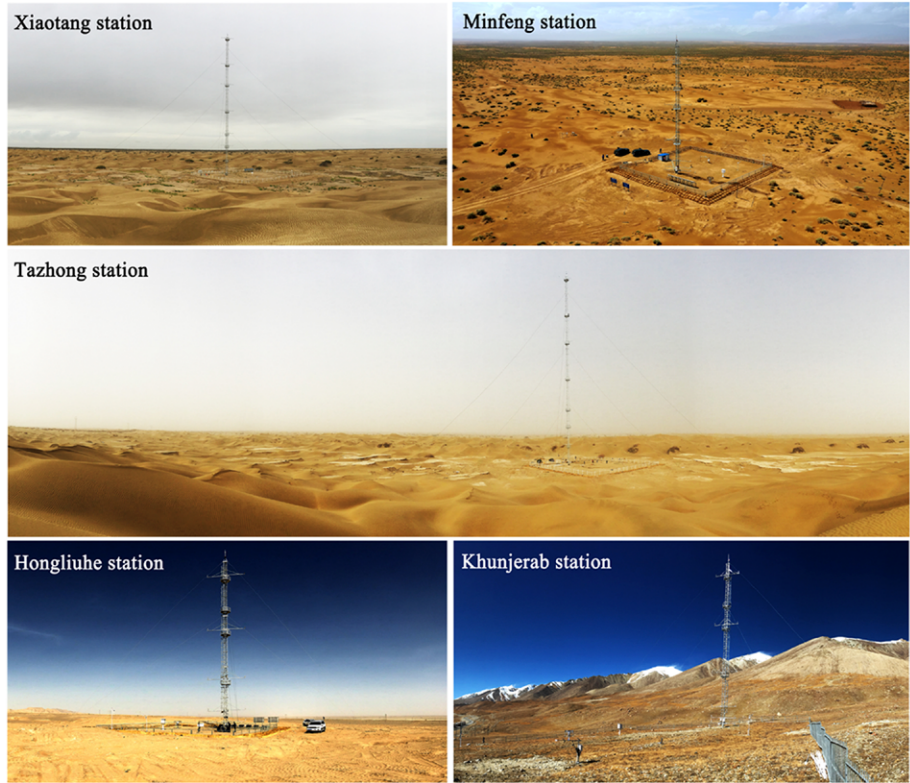
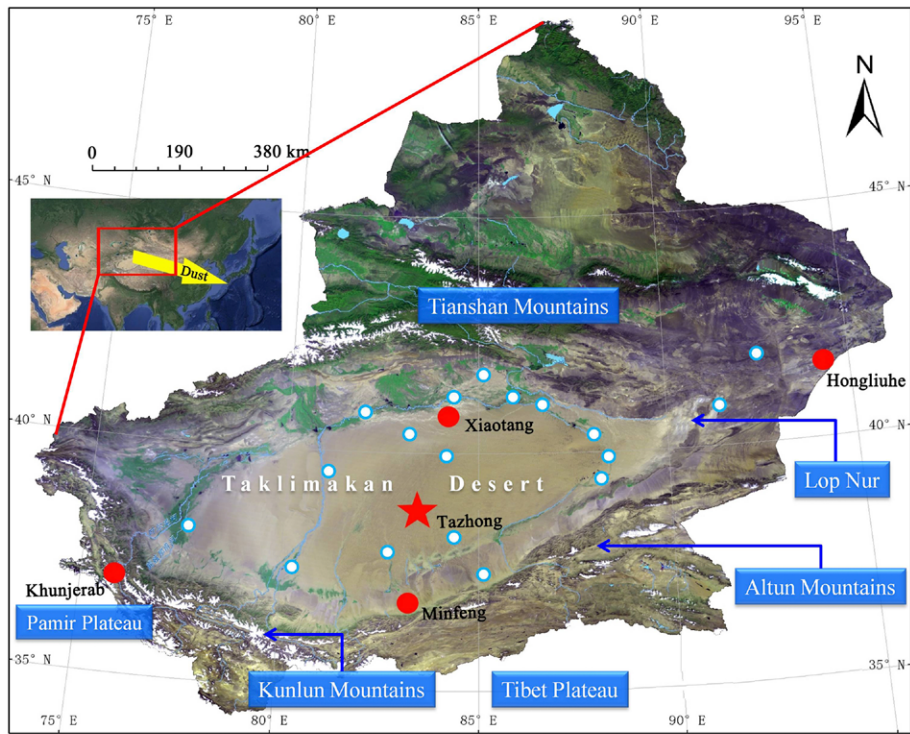


Fig. 1. Location and layout of the Desert Environment and Climate Observation Network (DECON) across the Taklimakan Desert (TD). The Tazhong station (longitude: $83^{\circ}39'E$; latitude: $38^{\circ}58'N$; altitude: 1,103 m), as the core of DECON, is located in the hinterland of the TD. The Xiaotang station (longitude: $84^{\circ}18'E$; latitude: $40^{\circ}49'N$; altitude: 932 m) and Minfeng station (longitude: $83^{\circ}10'E$; latitude: $36^{\circ}43'N$; altitude: 2,179 m) are located along the northern and southern edges of the TD. The Hongliuhe station (longitude: $94^{\circ}43'E$; latitude: $41^{\circ}32'N$; altitude: 1,579 m) and Khunjerab station (longitude: $75^{\circ}27'E$; latitude: $36^{\circ}50'N$; altitude: 4,605 m) cover the east and west sides, respectively, of the TD. The white dots represent the 18 automatic weather stations that gather additional dust-storm meteorological information.

desert weather and climate processes, dust-storm activities, dust emission and transportation mechanisms, boundary layer structure, land–atmosphere interactions, and desert carbon sinks and feedback to global processes in global shifting deserts. Therefore, the observation results of DECON provide a good representation of the basic characteristics of the entire TD area. Moreover, the establishment of DECON has mitigated the situation of outdated observation techniques and insufficient observation data in the past.

Scientific objectives. The DECON design aims at achieving the following four scientific objectives:

- 1) The mechanism of dust aerosol emission, transportation, and deposition in the TD along with its surrounding areas are determined, including the key parameters of dust emission, dust aerosol transmission paths, and budget relationship over the TD, so as to improve the simulation effects of dust-storm numerical prediction models. In addition, the identification of the mechanism also intends to examine the influence of the TD on dust aerosol cycle in East Asia and the world, as well as its impact on ecological environment and human activities.
- 2) Based on the observation experiments on the atmospheric boundary layer and land surface processes in the TD and its surroundings, the evolutionary mechanism of the desert atmospheric boundary layer and the characteristics of land surface processes are investigated, the characteristic parameters and parameterization schemes of boundary layer and land surface processes are resolved, land surface process models are improved, the simulation accuracy of numerical prediction models is improved, and the effect mechanism of the TD on regional circulation and local weather processes is evaluated. All of these factors are expected to provide an accurate representation of the dynamic influences of the TD on the weather and climate of central Asia and East Asia.
- 3) To study the response and feedback of dust storms, desert carbon sinks, and desertification to climate change in the TD and its surrounding areas; reveal the interactions between the TD and its surrounding areas, including oases, mountains, and the TP; improve the understanding of the TD at the meteorological and environmental level; assess its impact, mitigate potential environmental issues, and promote sustainable development.
- 4) To develop desert meteorological detection techniques, observation norms, and standards. And detection methods of disastrous desert weather event are researched and developed to promote the development and integrated application of special monitoring instruments in the desert environment and climate. Simultaneously, collaborative field testing is adopted to evaluate the application performance of atmospheric detection equipment and methods under extreme conditions.

Operation and measurements

Instruments and data quality control. At present, the Tazhong station mainly has an 80-m gradient meteorological tower, surface solar radiation monitoring instrument, land–atmosphere interaction monitoring instrument, boundary layer monitoring instrument, atmospheric composition monitoring instrument, wind and sand activity monitoring instrument, and data service platform. Table 1 and Fig. 2 provide detailed information on the instrumentation at the Tazhong station. In addition, with the advent of oil exploitation in the TB since the 1990s, many miniature artificial oases have been established in the TD to prevent dust-storm invasions and protect oil production systems. A 3-m land–atmosphere flux observation tower has been installed in the shelter forest of an oasis. This provides excellent experimental conditions for comparative research on microclimates, land–atmosphere interactions, and surface radiation between the shifting sand area and the artificial desert oasis. Additionally, the Tazhong station provides a reference for the establishment, management, and development of artificial desert oases.

Table 1. List of the core observation sensors and parameters of the Tazhong station.

Observation system	Observation variables	Instrument and equipment (model, manufacturer)	Installation instructions
80-m gradient meteorological tower	Gradient of the wind speed and direction	Anemometer (WindObserver II-65, Gill Instruments)	Sensors are installed at 0.5, 1, 2, 4, 10, 20, 32, 47, 63, and 80 m along the meteorological tower
	Gradient of the air temperature and humidity	Thermohygrometer (HMP155A, Vaisala)	Sensors are installed at 0.5, 1, 2, 4, 10, 20, 32, 47, 63, and 80 m along the meteorological tower
	Atmospheric pressure	Barometer (PTB330, Vaisala)	Sensor is installed at 1.5 m on the meteorological tower
	Gradient of the soil temperature	Soil thermometer (109, Campbell)	Sensors are installed at depths of 0, 5, 10, 20, and 40 cm in the sand
	Gradient of the soil moisture	Soil hygrometer (93640Hydra, Stevens)	Sensors are installed at depths of 5, 10, 20, and 40 cm in the sand
	Gradient of the soil heat flux	Heat flux plate (HFP01SC, Hukseflux)	Sensors are installed at depths of 5, 10, 20, and 40 cm in the sand
Surface solar radiation monitoring instrument	Total solar radiation	Total solar radiometer (SR20, Hukseflux)	Sensors are installed on a sun tracker (STR-22G, EKO)
	Atmospheric longwave radiation	Longwave radiometer (IR20, Hukseflux)	
	Ground-reflected radiation	Total solar radiometer (SR20, Hukseflux)	
	Ground longwave radiation	Longwave radiometer (IR20, Hukseflux)	
	Direct solar radiation	Direct solar radiometer (DR02, Hukseflux)	
	Scattered radiation	Total solar radiometer (SR20, Hukseflux)	
	UV-A and UV-B radiation	Dual-band ultraviolet radiometer (UVS-AB-T, Kipp and Zonen)	Sensors are installed at 1.5 m above the sand surface
	Photosynthetically active radiation	Photosynthetically active radiation radiometer (LI190SB, Campbell)	
Land-atmosphere interaction monitoring instrument	10-m gradient meteorological tower	Anemometer (WindObserver II-65, Gill Instruments), thermohygrometer (HMP155A, Vaisala), barometer (PTB330, Vaisala), soil thermometer (109, Campbell), soil hygrometer (93640Hydra, Stevens), and heat flux plate (HFP01SC, Hukseflux)	The 10-m gradient meteorological tower is installed in the shifting sand area about 1 km west of the 80-m gradient meteorological tower
			The anemometers and thermohygrometers are installed at 0.5, 1, 2, 4, and 10 m along the meteorological tower
			The barometer is installed at 1.5 m on the meteorological tower
			The soil thermometers are installed at depths of 0, 5, 10, 20, and 40 cm in the sand
			The soil hygrometers and heat flux plates are installed at depths of 5, 10, 20, and 40 cm in the sand
Sensitive heat flux, latent heat flux, water vapor flux, and CO ₂ flux	Eddy covariance instrument (IRGASON, Campbell)	The equipment is installed at 3 m above the surface of the shifting sand area and shelter forestland; in addition, an equipment set is installed at 10 m on the 80-m meteorological tower	
Soil CO ₂ flux	Automatic CO ₂ flux measurement instrument (LICOR-8100A + LICOR-8150)	Movable	
Boundary layer monitoring instrument	Wind speed and wind vertical profile	Wind profile radar (Arida3000Q, Beijing Elda)	Movable
	Air temperature and humidity vertical profiles	GPS meteorological sounding instrument (F1260, the 23rd Institute of China Aerospace Science and Industry Corporation) and captive balloon meteorological sounding instrument (DigiCORA, Vaisala)	Movable
	Aerosol concentration vertical distribution	Drone (M600 PRO, DJI), Thermohygrometer (Onset U12-011, HOBO), barometer (PTB330, Vaisala), and atmospheric particulate sampler (531S, Met One)	Movable
Atmospheric composition monitoring instrument	Atmospheric CO ₂ /CH ₄ /H ₂ O concentration	Greenhouse gas analyzer (GGA-24r-EP, LGR)	Movable

Table 1. (Continued).

Observation system	Observation variables	Instrument and equipment (model, manufacturer)	Installation instructions
Wind and sand activity monitoring instrument	Number of saltation grains	Sand impact sensor (H11B, Sensit)	Sensors are installed at 5 and 10 cm above the sand surface
	Horizontal sand fluxes	Automatic sand trap (CWHF, TRUWEL), BSNE sand trap (BSNE, TRUWEL) and microgradient sand trap (MST, TRUWEL)	Installed in the shifting sand area
	Weather phenomena	Weather phenomenon monitor (PWS100-XT, Campbell)	Install in the shifting sand area

In regard to the four satellite stations of DECON, given their design positioning and limitations of observation conditions, the observation equipment and experiments are the same but somewhat customized to each site. The Xiaotang station is equipped with a 100-m gradient meteorological tower, an eddy covariance instrument, a surface solar radiation monitoring instrument, and a wind and sand activity monitoring instrument. The Minfeng, Hongliuhe, and Khunjerab stations are equipped with a 35-m gradient meteorological tower, an eddy covariance instrument, a surface radiation monitoring instrument, and a weather phenomenon monitor. All of these instruments have been carefully selected and operate in the automatic mode for observation tasks in harsh environments.

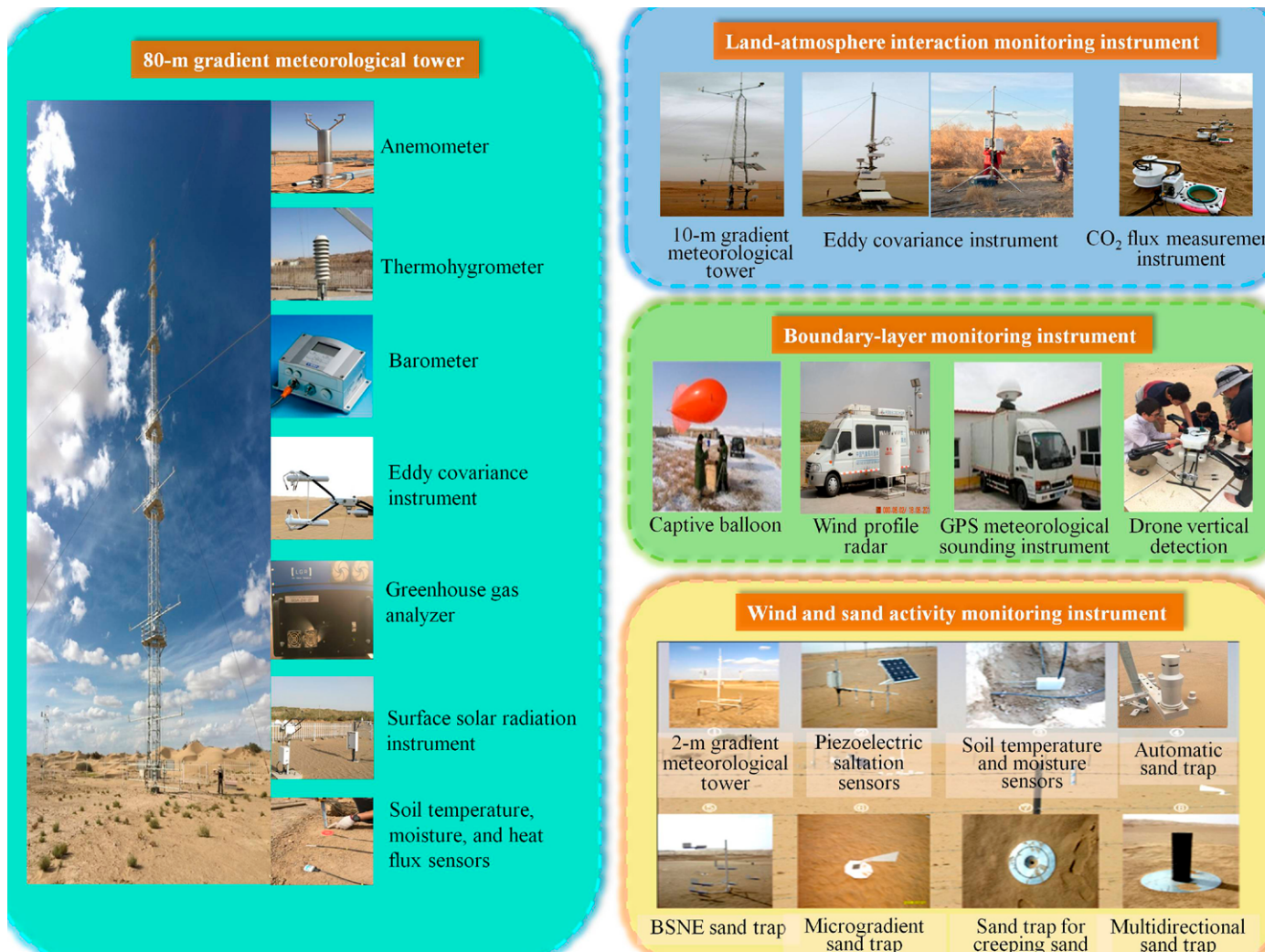


Fig. 2. Structure of the Tazhong station and the main instruments.

The main goal of data quality control is to reduce low-quality observation data as much as possible to obtain real scientific observations (Ma et al. 2020). All of the DECON instruments operate in extremely harsh desert environments. Many of these conditions exceed expectations, and the observation instruments are usually pushed to their operating limits. Here, we provide examples of the extremes encountered. 1) The average grain size of the surface shifting sand in the TD only ranges from 0.083 to 0.129 mm (Huo et al. 2011; Yang et al. 2016b). This fine sand is easily blown from the desert surface, causing frequent strong dust storms in the TB. When fine sand particles enter an instrument, they could cause abrasions, blockages, and corrosion of mechanical parts. These fine particles tend to block the light path of photosensitive sensors, thus reducing the measurement accuracy of these instruments. 2) The desert surface exhibits a high fluidity; hence, fine sand particles readily accumulate and erode surfaces. Moreover, the shifting sand changes the measuring positions of the sensors. In addition, the low heat capacity and extreme dryness of the shifting sand may cause abrupt changes in the soil temperature. For example, the daily variation in the surface temperature is 53°C, and the maximum surface temperature during the day reaches 78°C at the Tazhong station. This exceeds the optimal environmental conditions for certain sensors and reduces the sensor sensitivity. 3) The extremely low air humidity, intense solar radiation, and high salinity and alkalinity of the sand cause aging, corrosion, and static electricity in the sensors' electronic components, which affects the measurement results. Therefore, the above severe environmental conditions and technical limitations require that strict quality control measures are in place for DECON observation data through standard procedures. Data quality control consists of three stages: instrument status inspection for abnormalities, data index inspection, and variance inspection based on a moving window. The first stage involves evaluating whether the instrument state is normal, examining the data continuity, directly removing any data obtained in the abnormal instrument state, and explaining discontinuous data periods. In the second stage, according to the characteristics of the sensor itself and past historical observation data, the quality control involves establishing the quality control range, comprehensively assessing the rationality of the data, and eliminating data spikes. In the third stage, the variance in the observation data are analyzed based on a moving window. In the verification process, a corresponding variance threshold is set according to the characteristics of the different variables. In addition to these automatic quality control measures, researchers also need to further screen data for issues related to their particular research projects.

IDM has attempted to reduce sensor damage and inaccuracy by optimizing the measurement techniques used in DECON operation. For example, all mechanical anemometers have been replaced with ultrasonic anemometers, and sealing rubber rings or sealed chambers have been added to avoid abrasion, blockage, and corrosion of mechanical components caused by dust entering the instruments. In regard to the soil monitoring system, by setting a fixed zero plane and sand barrier on the surface of the shifting sand, the sensor positions in the sand can be maintained at a fixed position. In addition, transmission cables are protected from corrosion and aging by protective tube encapsulation and deep burial of the cables/tubes.

Operation and maintenance. IDM is responsible for all operations, maintenance, and management of DECON. To ensure the continuity and accuracy of the various observation data acquired at the Tazhong station, the data service platform is custom equipped for monitoring, storage, quality control, transmission, and retrieval. Onsite personnel are responsible for daily inspections, maintenance, and data monitoring of all observation instruments. The Tazhong station observations cover an area of 37,410 m². Except for the observation equipment, office apartments equipped with experimental and living facilities covering 300 m² are present to maintain all necessary support, including life support, for the researchers who conduct experiments at the observation station. The remaining four satellite stations are equipped

with automatic observation equipment powered by solar energy. They are monitored by local meteorological bureaus (please refer to Fig. 1).

Data transmission in DECON relies on the general packet radio service to transmit to the data service platform of IDM. The platform realizes real-time monitoring, quality control, storage, and retrieval of all data obtained from DECON. Additionally, to further reduce the probability of data drift or observation equipment failure in the rather harsh environment, we adopt a management mode similar to that of the Tibetan Observation and Research Platform atmosphere–land interaction (Ma et al. 2008, 2017). Every two months, two professional technical maintenance personnel travel to each DECON observation station to perform comprehensive maintenance (cleaning, repair, and calibration) of all onsite equipment and verify the remote real-time monitoring operations. If instrument failure or data abnormalities are found, the technical maintenance personnel work to immediately resolve any issues.

Main observational results

Dust-storm observations. Dust storms in the TB region may last longer than 10 days on average each year, and there are two active centers, at which dust storms have lasted for longer than 30 days, including Xiaotang with a record of 47 days and Minfeng with a record of 33.6 days. Moreover, the dust-storm events in the TB exhibit a fluctuating downward trend (please refer to Fig. 3; Yang et al. 2016a). As shown in Fig. 4a, the main paths leading to dust storms in the TB include north, east, and west routes. Among them, the dust-storm intensity in the TB along the north and east routes tends to be relatively high.

As an example, we show the strong mixed-dust weather event along the north and east routes in the TB captured by DECON from 25 to 28 July 2019, in Fig. 4. Except for the Hongliuhe station, the other stations also recorded this dust weather event, and the highest dust-storm intensity readings were recorded at the Tazhong station. In addition, due to the spatial location of the stations and dust-storm development, the response time of each station to the dust storm revealed an obvious sequence. Among them, the Xiaotang station was the first to respond to the dust storm, followed by the Tazhong station. In the regions surrounding the Tazhong and Xiaotang stations, with a rapid increase in wind speed and notable decline in visibility, strong dust storms quickly engulfed the sky, and the maximum instantaneous wind speed at the Tazhong station was 21.84 m s^{-1} , while the minimum visibility was 300 m. When the dust storm reached the Minfeng region, the wind speed had decreased, as it was obstructed by the Kunlun Mountains. Sand and dust particles entrained by the dust storm were intercepted in this area, resulting in a strong dust storm with a low wind speed in Minfeng and floating dust over the next few days. In addition, the strong dust storm extensively transported floating dust to the Pamir Plateau with an average altitude higher than

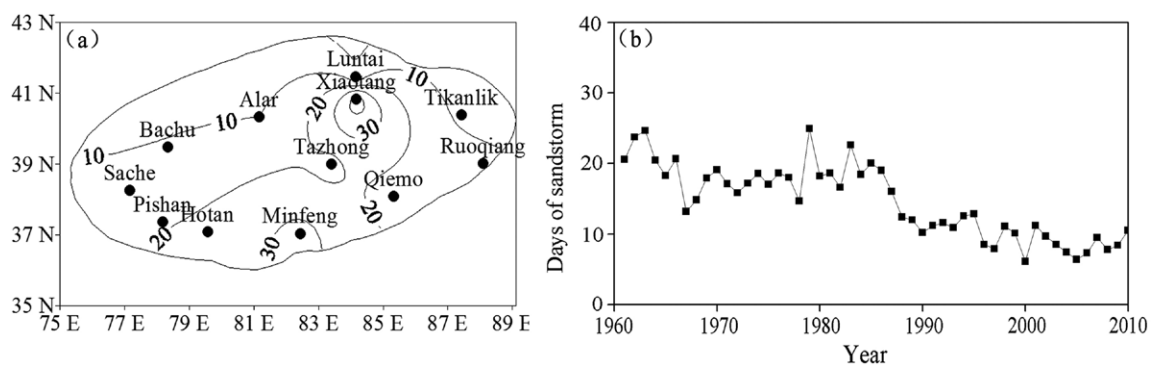


Fig. 3. Spatial and temporal variations in the annual mean days of dust-storm activity in the TD (Yang et al. 2016a). (a) Spatial variation. The points with the same dust-storm days are on the same contour line. (b) Temporal variation.

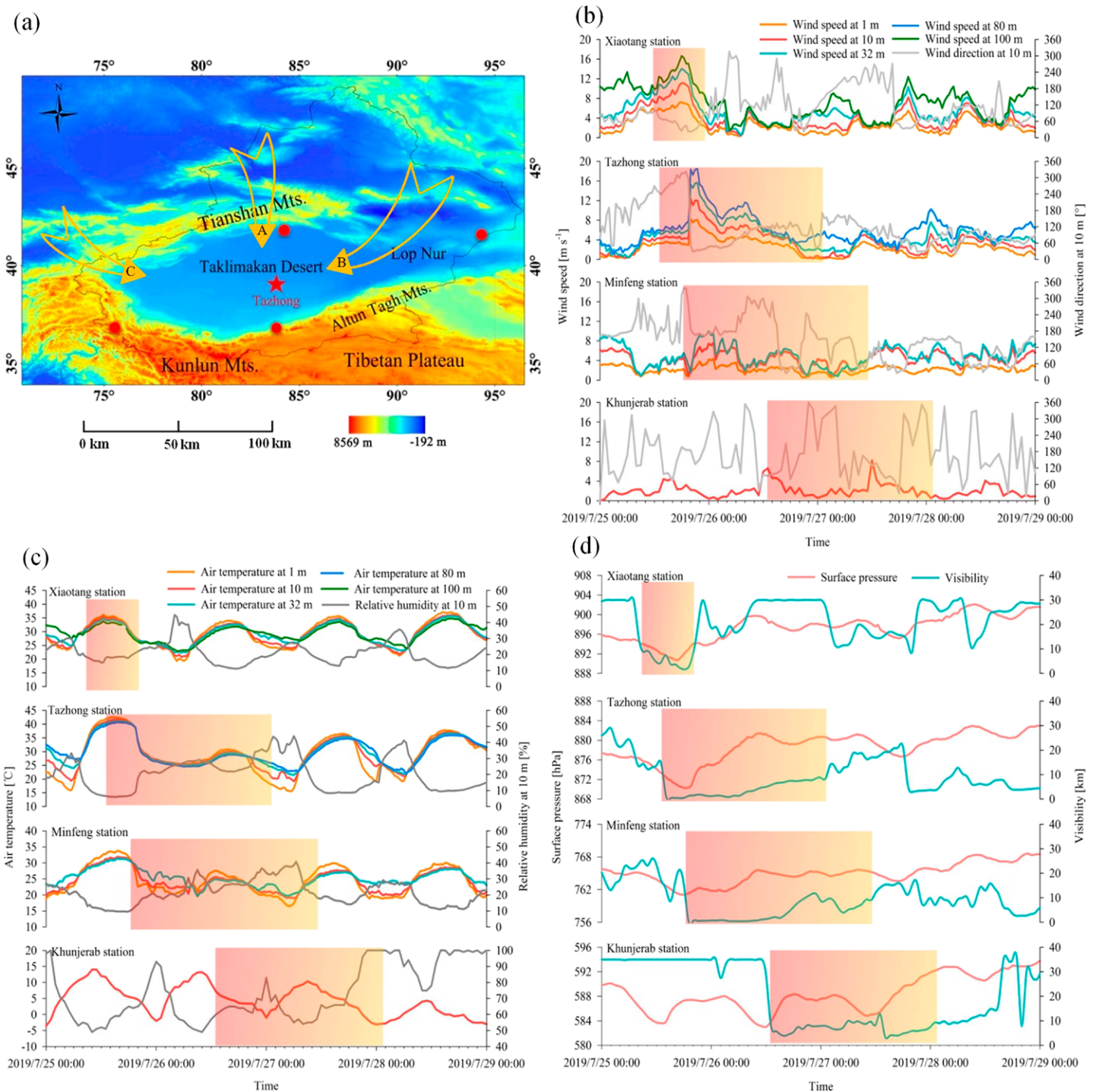


Fig. 4. (a) Routes of the weather systems causing dust storms in the TB entering the basin: A, north route (the weather system climbs over the Tianshan Mountains and enters the TB); B, east route (the weather system goes around to the low-altitude eastern region of the TB and then flows back into the basin); and C, west route (the weather system climbs over the Pamir Plateau and enters the TB). The time series of the (b) gradient wind speed and wind direction, (c) gradient of the air temperature and relative humidity, and (d) surface pressure and visibility during a strong dust weather event in the TB observed by DECON from 25 to 28 Jul 2019. Due to a lightning strike before this dust weather event, only the anemometer and thermohygrometer at 10 m of the gradient meteorological tower of the Khunjerab station operated normally during this dust storm. The color shadow indicates the occurrence period of the dust weather event with a visibility lower than 10 km.

4,000 m. This clearly proves that dust aerosols from the TD may ascend to the Pamir Plateau or the TP under strong dust weather conditions and may impose a series of profound effects on the plateau concerning its cloud cover, precipitation, surface energy distribution, and ice

and snow melting characteristics (Huang et al. 2007, 2008, 2017; Liu et al. 2011; Ge et al. 2014; Liu et al. 2019, 2020a,b). On this basis, combined with satellite remote sensing, remote sensing monitoring data on dust storms can be verified by DECON. Improvements continue to be made to the observation network to expand its application range.

Surface dust emission observation. Since 2008, at the Tazhong station, simultaneous observation experiments have been performed on the sand particle activity, micrometeorology, and surface soil environment of the shifting sand in the TD. Figure 5 shows dust emissions consisting of TD shifting sand during the observed dust weather event from 25 to 26 July 2019. Wind is commonly the main factor causing the movement of sand particles across the surface, and the relationship between these aspects is an exponential function (Fig. 5b). In the TD, when the wind speed reaches the threshold velocity of 4.15 m s^{-1} during a dust storm, the sand particles on the surface become entrained. At a wind speed of 8 m s^{-1} and beyond, the number of saltation sand particles sharply increases with the wind speed. Apart from continuous monitoring of surface dust emissions at the Tazhong station, new equipment and technology developments are developed to sharpen the research capacity of the station. Figure 6a shows a time series of the sediment weight collected in the shifting sand area of the Tazhong station in May 2015 by our custom-designed automatic sand trap; design and description details of the automatic sand trap have been provided by Yang et al. (2017a); this instrument provides the first real-time automatic measurement of the horizontal sand flux at different heights and has the function of sand sample collection. Moreover, this instrument can be used in combination with key environmental measurement systems (such as those for the measurement of the wind speed, saltation sand particle content, air temperature, and soil moisture) to obtain more dust emission details during dust weather events for the optimization of parameterization schemes representing dust emissions. Figure 6b reveals that seven dust emission events occurred in the Tazhong area in May 2015. During each event, the horizontal dust flux exponentially decreased with increasing height, and nearly 50% of the dust transport was concentrated within 30 cm above the surface. These results could guide the selection of sand control strategies and the implementation of sand control projects in the TD. Additionally, with the use of the relationship between the total horizontal dust flux and the total number of saltation sand particles at 5 cm during the above seven dust events

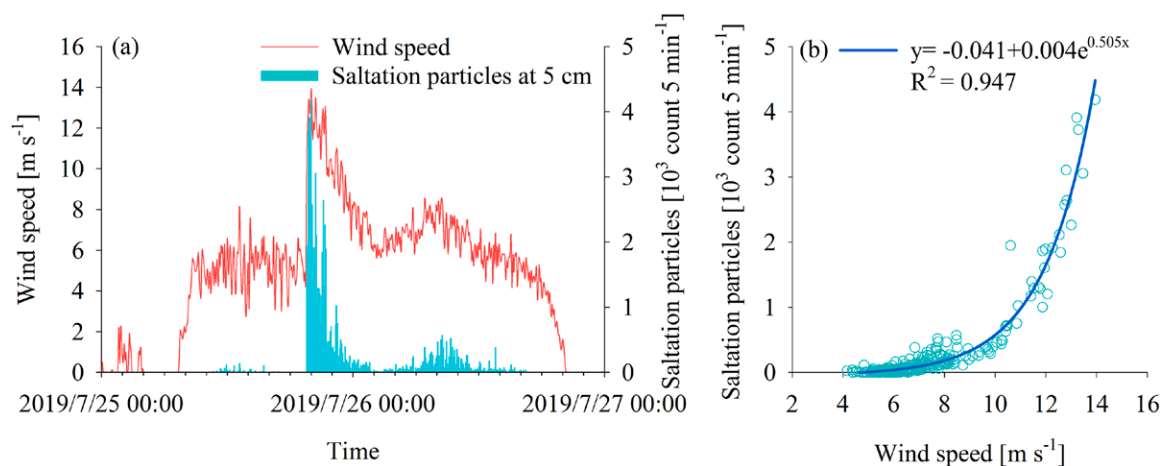


Fig. 5. (a) Time series of the 5-min average wind speed at 2 m and the 5-min saltation sand particles at 5 cm in the shifting sand area during the dust weather event that passed through the Tazhong area from 25 to 26 Jul 2019. (b) The regression relationship between the 5-min average wind speed at 2 m and 5-min saltation sand particles at 5 cm in the Tazhong shifting sand area during the dust weather event.

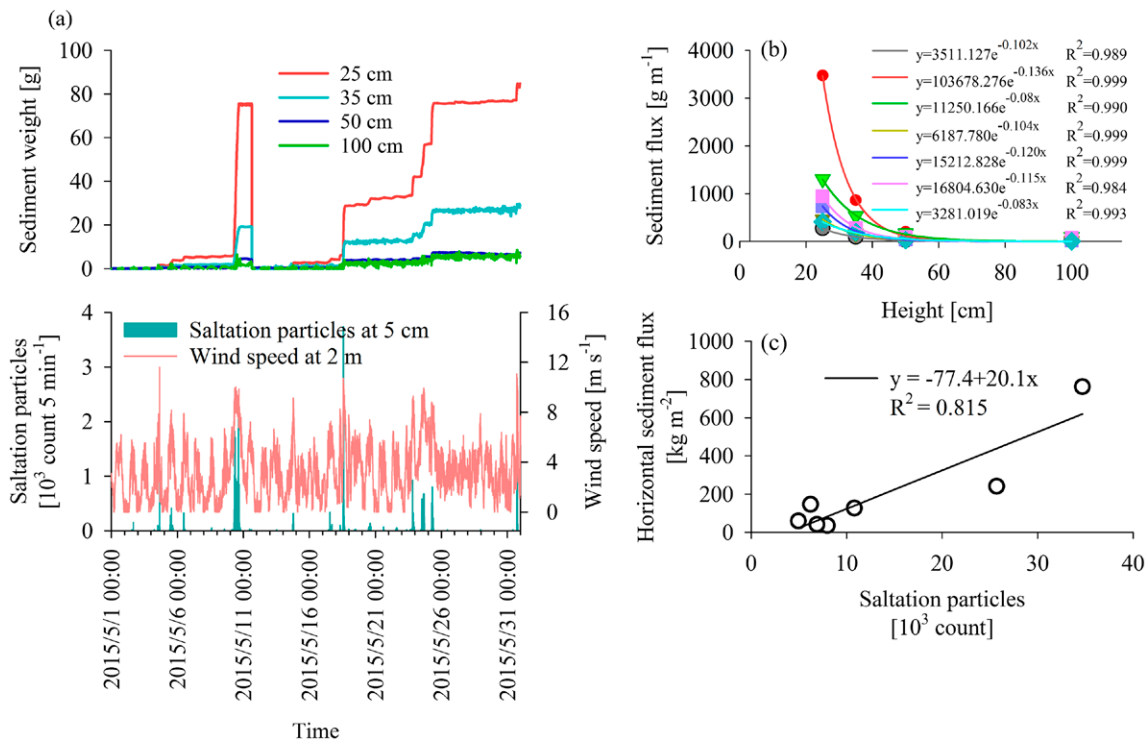


Fig. 6. (a) Time series of the sediment weight determined by the automatic sand trap at different heights and the corresponding 5-min average wind speed at 2 m and number of saltation sand particles at 5 cm in the shifting sand area of Tazhong station in May 2015. (b) In May 2015, the regression relationship between the sediment flux of seven dust emission events and the corresponding height. (c) Based on the integration of the aforementioned seven exponential functions, we obtained the total horizontal sediment flux over a $1 \text{ m} \times 1 \text{ m}$ cross section in the shifting sand area during each dust emission event. The regression relationship between the total horizontal sediment flux over the $1 \text{ m} \times 1 \text{ m}$ cross section and the total number of saltation sand particles at 5 cm was established.

(Fig. 6c), the real-time estimation of the horizontal dust flux across a $1 \text{ m} \times 1 \text{ m}$ section of the surface could be realized. It was estimated that the dust weather conditions during the event from 25 to 26 July 2019, resulted in a horizontal dust flux of 1,498,942 kg across the surface of a $1 \text{ m} \times 1 \text{ m}$ section in the area surrounding the Tazhong station.

The soil moisture is another important factor influencing dust emissions. On the one hand, the increase in soil moisture increases the cohesive force between soil particles and inhibits the occurrence of dust emission. On the other hand, the increase in soil moisture promotes the accumulation of small dust particles into larger aggregates and alters the particle size distribution of the shifting sand; this could lead to a reduction in dust emissions (Yang et al. 2020). Therefore, in recent years, numerous observation experiments conducted at the Tazhong station have provided data on the influences of the soil moisture and soil temperature on the dust emission process in the TD (Yang 2019; Yang et al. 2020). Moreover, combined with wind tunnel simulation experiments, parameterization schemes of the influences of soil moisture on the threshold value of dust emission initiation and horizontal and vertical dust fluxes have been established and modified (Yang 2019). These models are expected to provide a foundation for the further optimization of localized dust emission parameterization schemes and dust weather forecasting accuracy in the TD.

Structure of the atmospheric boundary layer. Based on analysis of encrypted sounding data measured at the Tazhong station from 24 to 28 July 2019 (Fig. 7), the turbulence

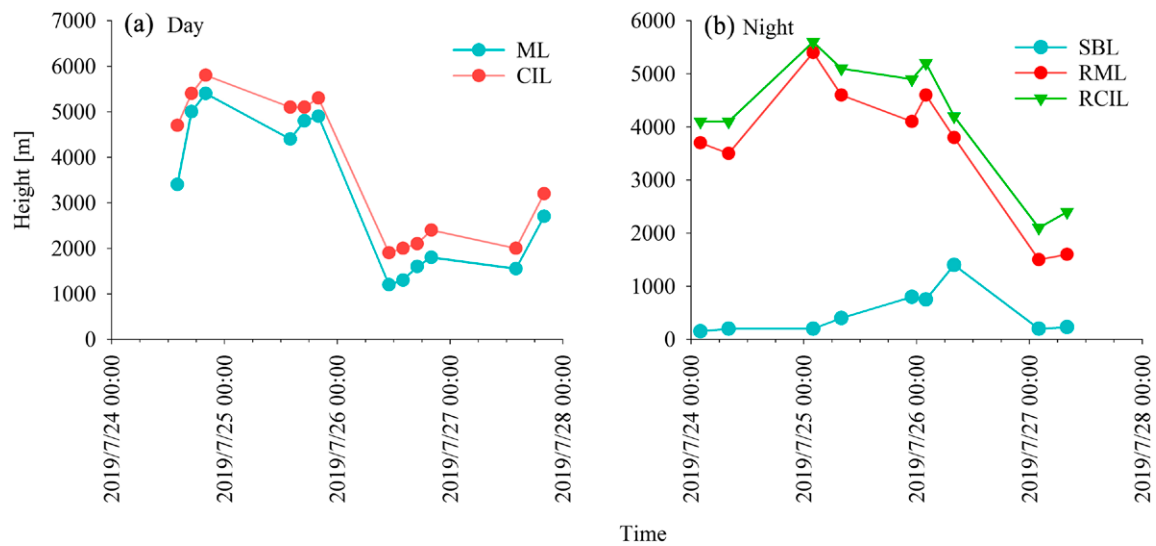


Fig. 7. Variation characteristics of the atmospheric boundary layer structure in the hinterland of the TD from 24 to 28 Jul 2019. (a) Time series of the thickness of the mixed layer (ML) and the capping inversion layer (CIL) during the daytime. (b) Time series of the thickness of the stable boundary layer (SBL), residual mixed layer (RML), and residual capping inversion layer (RCIL) at night.

in the hinterland of the TD was very high under clear-sky conditions in summer, and the convective boundary layer developed into an extremely thick layer during the daytime, reaching a maximum thickness of 5,400 m. This thickness is close to that observed in the Sahara Desert (Marsham et al. 2008). The residual mixing layer at night continued the thick convective mixing layer developed during the daytime, with a maximum height of 5,400 m, whereas the thickness of the stable boundary layer (SBL) at night only reached approximately 300 m. The dust storm that occurred at night on 25 July 2019, imposed a major impact on the atmospheric boundary layer. The thickness of the convective boundary layer was reduced to 1,200 m during the daytime, the height of the residual mixed layer (RML) at night also decreased, and the SBL at night increased to 1,400 m. As the impact of the dust storm gradually faded, the structure of the atmospheric boundary layer eventually returned to its clear-sky state.

Figure 8 shows the changes in the atmospheric boundary layer in more detail before and after the dust storm. During the transit period of the dust storm, a cold air mass with a thickness of approximately 1,000 m entered the area, at a maximum wind speed of 24.3 m s^{-1} . This cold air mass effectively destroyed the stable nighttime structure of the boundary layer and removed the inversion layer on the surface, while the RML remained at high altitudes. After the dust storm, the boundary layer structure gradually recovered. However, the dust particles suspended in the atmosphere reduced the solar radiation reaching Earth's surface, which to a certain extent inhibited the recovery of the convective boundary layer during the day and the SBL at night. Additionally, under clear-sky conditions in the desert, a low-level jet stream occurred caused by the inertial oscillations at night. The speed of the jet stream gradually increased after sunset, reaching its maximum speed at midnight, and then basically collapsing after sunrise.

In recent years, Wang et al. (2017, 2018) conducted boundary layer observation experiments during dust storms using a wind profile radar at the Tazhong station. Their results revealed clear dust-storm traces in the radar echo intensity, which could be adopted to assess the transport height and mass concentration of dust (Fig. 9). Based on this effort, a new method of quantitative dust-storm monitoring using the wind profile radar was established.

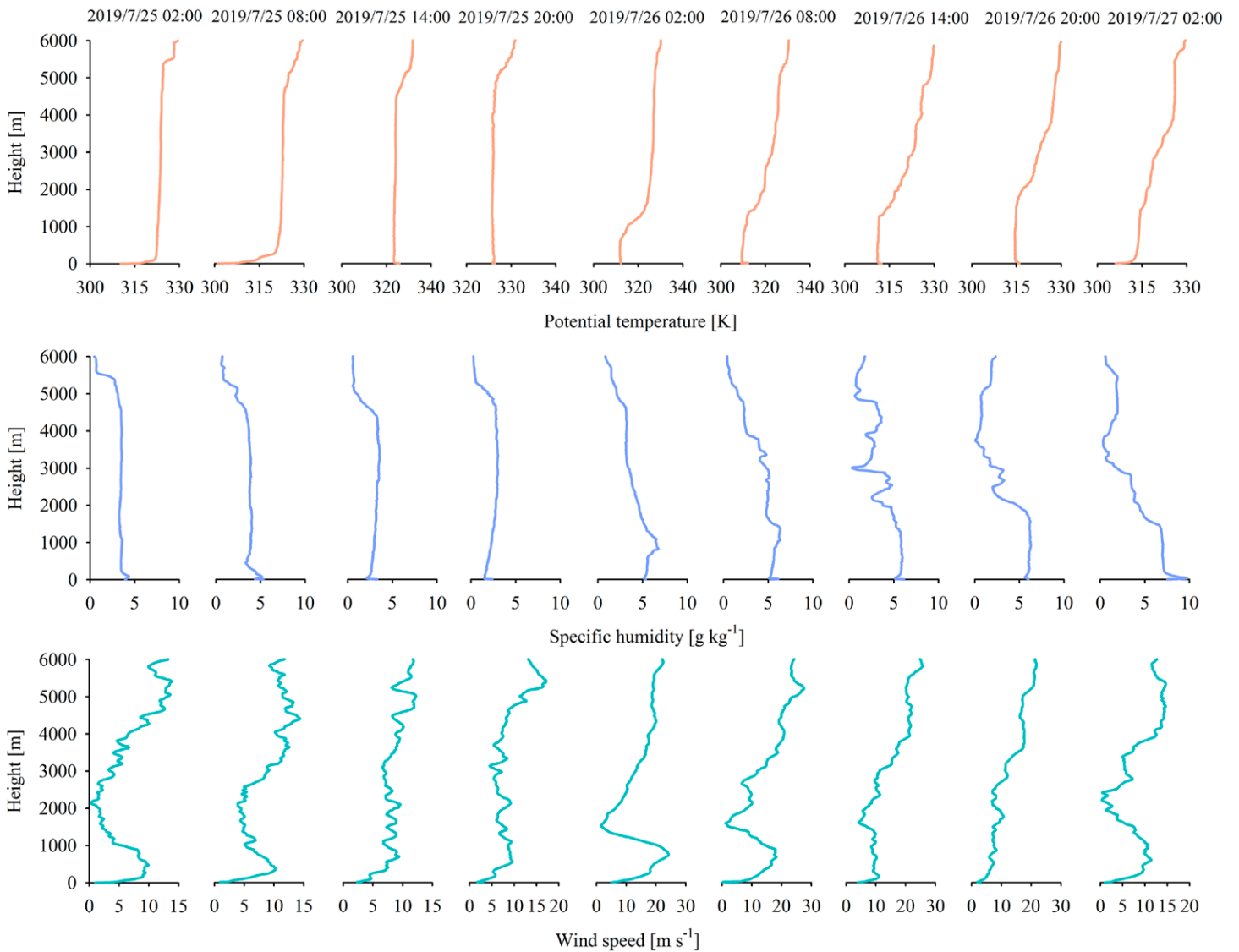


Fig. 8. Time series of the vertical profiles of the (a) potential temperature, (b) specific humidity, and (c) wind speed in the hinterland of the TD from 25 to 27 Jul 2019.

Turbulent fluxes and land surface parameters. Compared to other ecosystems, the land surface process characteristics of desert ecosystems exhibit obvious particularities. Based on the open-path eddy correlation of each station in DECON, the turbulence fluxes (momentum flux, sensible heat flux, latent heat flux, and CO₂ flux) in the TD and its surrounding areas and the land surface parameters of the Tazhong area (aerodynamic roughness length, thermal roughness length, albedo, and surface emissivity) were analyzed. These results provide the information necessary to improve the simulation ability of land surface models for desert ecosystems.

TURBULENCE FLUXES. As shown in Fig. 10, the momentum fluxes of each station reveal a distinct diurnal variation and seasonal fluctuation. Generally, the momentum flux is low at night, increases after sunrise, and reaches a daily peak in the afternoon. The momentum fluxes of each station in spring and summer are higher than those in autumn and winter. Moreover, the momentum flux of the Khunjerab station is higher than that of the other stations. These discrepancies are related to the geomorphic environment and wind speed at each station. Generally, an uneven geomorphic environment and high wind speed will lead to a high momentum flux. The frequent dust weather events in spring and summer in the TD also

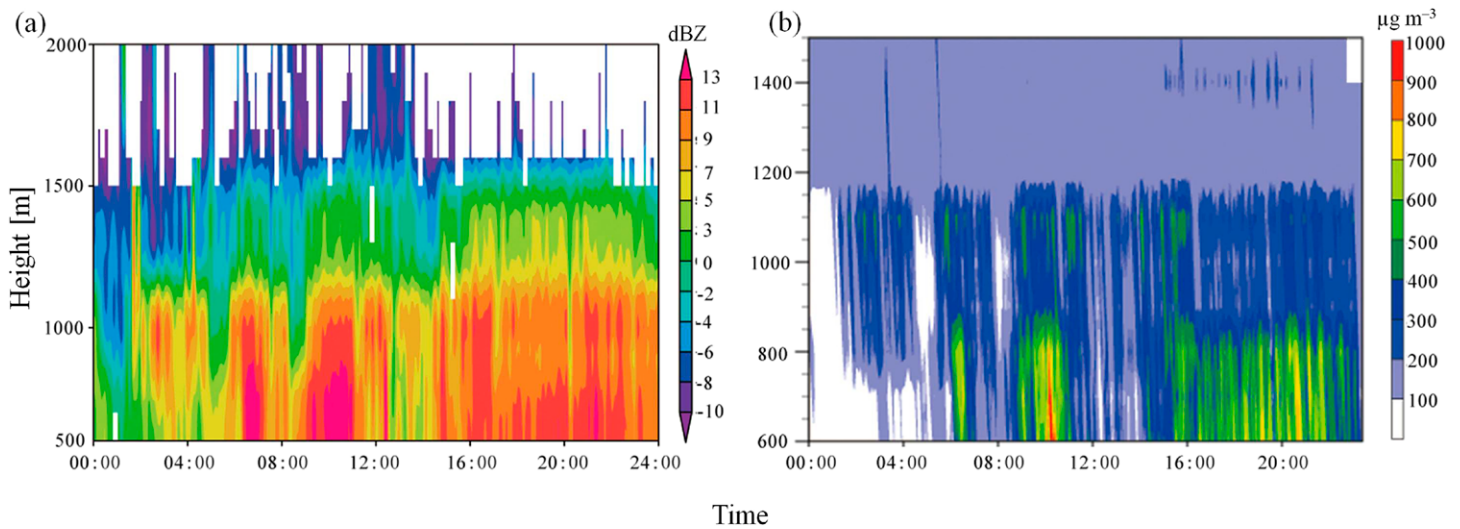


Fig. 9. Time–height profiles of the (a) dust weather echo intensity (dBZ) and the (b) particle concentration ($\mu\text{g m}^{-3}$) during the dust event on 23 Apr 2014, measured with a wind profile radar (Wang et al. 2017).

confirm the fact that the momentum flux is relatively high in these seasons. In addition, Khunjerab is located in a high-altitude mountain area, where the year-round high wind speed and uneven geomorphic environment result in a high momentum flux.

The sensible and latent heat fluxes of each station exhibit obvious diurnal and seasonal variations. The sensible heat flux is the main consumption form of surface energy due to the extremely arid desert climate, whereas the latent heat flux is relatively low. The increase in summer precipitation in the desert results in a slight increase in the latent heat flux. However, this does not fundamentally alter the situation whereby the sensible heat flux is the main energy consumption form in this desert ecosystem.

As the Khunjerab and Minfeng stations are located in the mountainous area, which is on the edge of the TD, the altitude of the two stations is relatively high. Consequently, the precipitation and latent heat flux of them are higher than those of desert. Sparse shrubs occur around the Khunjerab and Minfeng stations. Plant photosynthesis and respiration result in a negative CO_2 flux during the day and a positive flux at night. This process is strengthened in the period of vigorous vegetation growth in summer and is very weak in winter. However, the Tazhong, Xiaotang, and Hongliuhe stations without vegetation coverage also exhibit similar daily CO_2 flux dynamics. This unconventional phenomenon was also discovered in the deserts of Mexico (Hastings et al. 2005) and the United States (Wohlfahrt et al. 2008) in the early twenty-first century. Moreover, this triggered a wave of research on carbon sinks in deserts (Stone 2008; Ma et al. 2013, 2014; Li et al. 2015; Fa et al. 2016). In recent years, we have applied an automatic soil respiration measurement system (LICOR-8100A) to determine the internal processes and main driving mechanism of the carbon sink in the TD for the first time through field observations and laboratory experiments. This information is useful for the prediction of the long-term trends of desert carbon sinks under climate change (Yang et al. 2017b, 2020a,b). Interestingly, the results of the daily change in the CO_2 flux obtained by the LICOR-8100A instrument and the open-path eddy covariance system in desert areas without vegetation cover did not correspond at all. After comprehensive testing of the LICOR-8100A instrument in the desert ecosystem, we gradually began to doubt the readings of the open-path eddy covariance system. Here, we speculate that the open-path eddy covariance system is quite susceptible to the extreme environment of the desert, which may be the main reason for the erroneous high CO_2 absorption reading in the desert. This has become one of our future research topics.

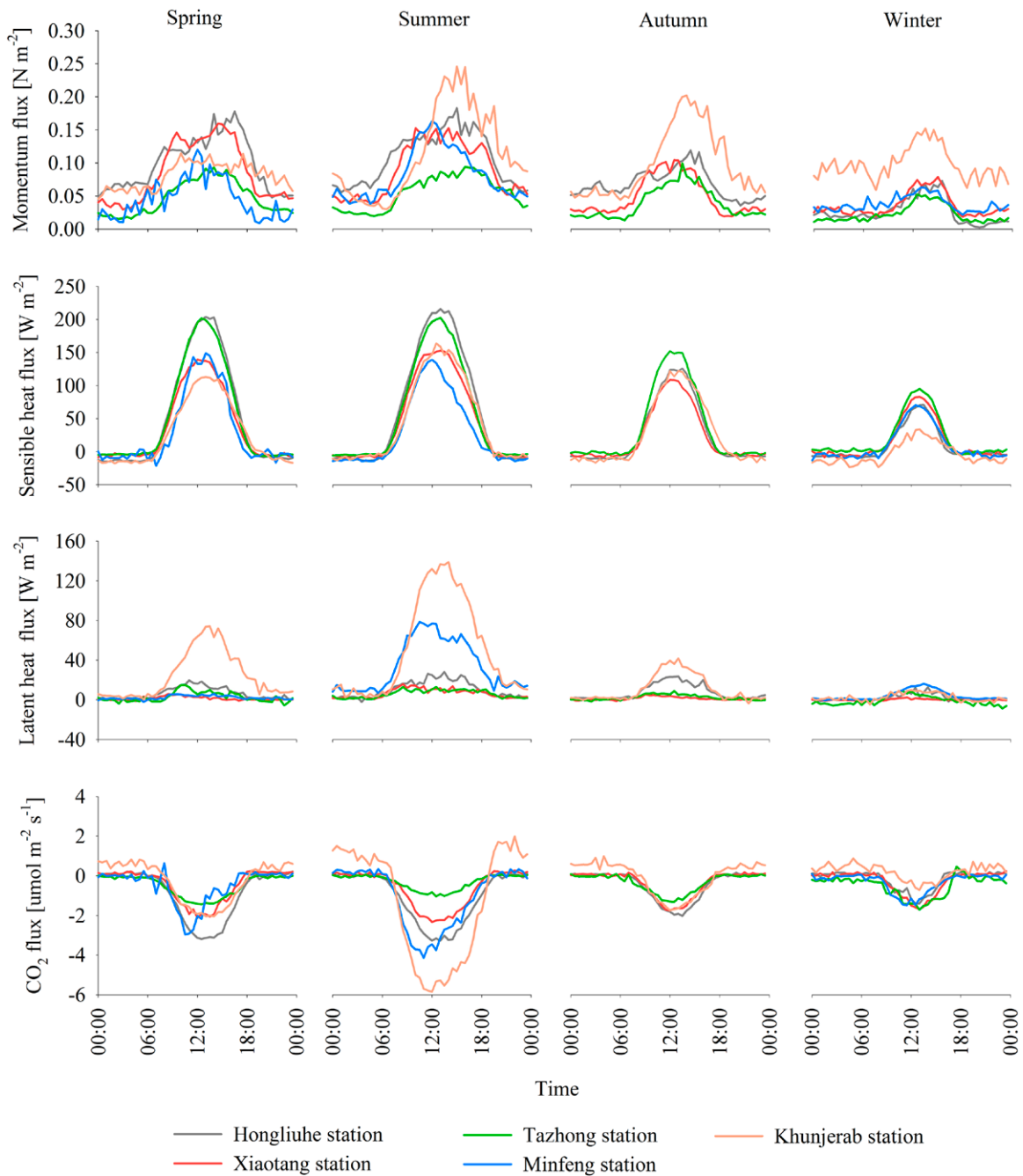


Fig. 10. Average daily variation in the momentum flux, sensible heat flux, latent heat flux, and CO_2 flux of the five DECON stations during the different seasons in 2019. Due to a power supply outage in the eddy covariance instrument in autumn 2019 at the Minfeng station, a large amount of flux data was missing, and the autumn flux data of the Minfeng station are not displayed.

LAND SURFACE PARAMETERS. The aerodynamic roughness length (Z_{om}) and thermal roughness length (Z_{oh}) are two key surface parameters for turbulent flux calculations with weather and climate models (Wang et al. 2016). In the hinterland of the TD Z_{om} is estimated to be 3.11×10^{-3} m, which is inversely proportional to the wind speed. Figure 11a shows the parameterization relationship between Z_{om} and wind speed. The thermal roughness length Z_{oh} exhibits obvious diurnal variation characteristics. Through comparative analysis, the Y07 parameterization scheme of Z_{oh} proposed by Yang et al. (2007) systematically improves the simulation effects of land surface models in terms of the surface temperature and sensible heat flux in arid areas. Moreover, it is also more suitable for the hinterland of the TD (Liu et al. 2012). In regard to the albedo, the most important factor is the solar elevation angle due to the low annual

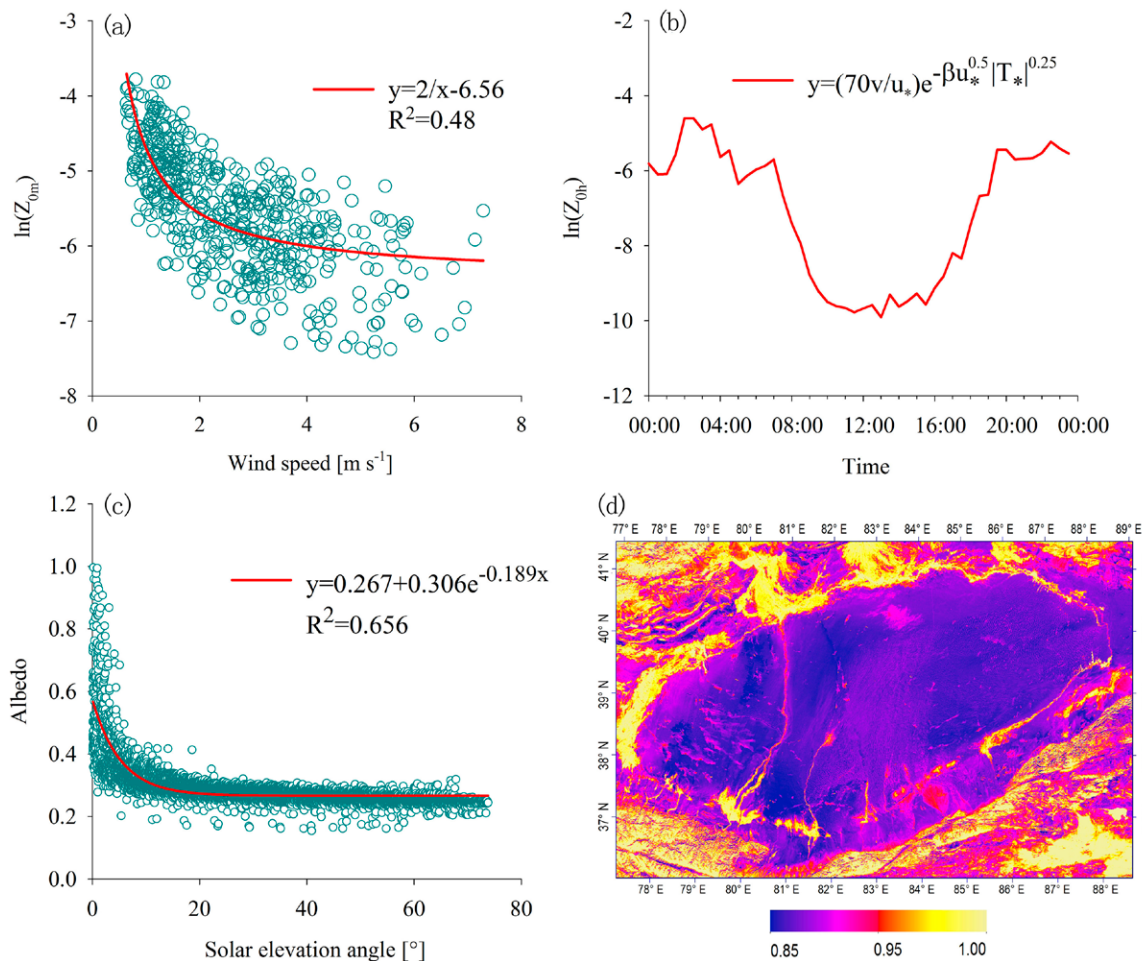


Fig. 11. Land surface parameters of the TD. (a) The inverse relationship between $\ln(Z_{0m})$ and wind speed, where Z_{0m} is the aerodynamic roughness length. (b) The Y07 parameterization scheme of Z_{0h} proposed by Yang et al. (2007), which is suitable for arid areas, where Z_{0h} is the thermal roughness length. (c) The exponential function relationship between the albedo and solar elevation angle. (d) The surface broadband emissivity of the TD and its surrounding areas obtained with the empirical method proposed by Li et al. (2016).

variation in the desert surface. After calculations, the annual albedo in the hinterland of the TD amounted to 0.27 ± 0.003 , and the parameterization relationship between the albedo and solar elevation angle is shown in Fig. 11c. In addition, based on observation of the surface spectrum in the TD and combined with the emissivity product of the Moderate Resolution Imaging Spectroradiometer (MODIS), Li et al. (2016) proposed an empirical method to estimate the surface broadband emissivity. The surface emissivity of the TD ranged from 0.88 to 0.91, that of the oasis ranged from 0.95 to 0.98, and that of the Tazhong area was 0.905. These land surface parameters and parameterization schemes were applied to a land surface model, which improved the simulation effects of the desert land surface to a certain extent.

Data availability and cooperation

For a long time, humans have felt distanced from the desert ecosystem, where life appears to be almost extinct, both physically in terms of its geography and the minimum occurrence of societal and cultural influences. Even in today's era of advanced technology, the desert ecosystem is still a great obstacle to human activities. In recent years, humans have developed an appreciation for the abundant mineral, light and heat resources in deserts, and the important roles deserts play in carbon sequestration, groundwater storage, and global material circulation, thus effectively shortening the distance between desert ecosystems

and humans. However, the lack of the most basic observation data of the desert ecosystem hinders its further understanding. The extreme environmental conditions make it more difficult to obtain basic observation data. In particular, the lack of a long-term standardized meteorological monitoring network has limited the understanding of the environment and climate of the desert ecosystem, not to mention the assessment of the desert impact, disaster prevention, and sustainable development.

As the second-largest shifting sand desert in the world, the TD is a typical representative of aeolian landforms in arid regions and is an important source of global dust aerosols. It directly affects the ecological environment and human health of East Asia in its entirety. After 20 years of effort, the establishment of DECON has resolved the situation of outdated observation techniques and insufficient observation data in the past. Through the cooperation of multiple stations, the resulting refined and abundant observation data are expected to play a key role in future scientific research efforts in regard to data support, monitoring, modeling, forecasting, and mitigation efforts involving dust-storm disasters, dust emission and transportation, desert land–atmosphere interactions, desert boundary layer structure, and desert carbon sequestration, with optimal parameterization schemes for modeling. It is our sincere hope that DECON will continue to promote cooperation and exchange with international organizations and within the science community regarding desert environment and climate research based on this platform. As such, we welcome participation from the scientific community worldwide in investigations and field experiments conducted in the TD. The observation data obtained from DECON are available to the public through the data-sharing website (www.crensed.ac.cn/portal/metadata?current_page=1&org=Taklimakan+Station), and the data are continuously updated for optimal information delivery as scientific efforts with the DECON framework progress. Through bilateral cooperation promoting the sharing of observation data and instruments, further research can be performed on the occurrence mechanism of disastrous weather events, the interaction between the TD and TP, desert convective heat bubbles, dust aerosol radiation effects, dust impact on clouds and precipitation, improvement of numerical dust-storm simulation, remote sensing product ground validation, and dust impact assessment on human health and living environments to maximize the research and demonstration value of DECON. Finally, DECON is expected to improve the environmental and meteorological support capacities of central Asia to meet the scientific and technological needs of desert ecosystems and the sustainable socioeconomic and cultural development of this region.

Acknowledgments. Fan Yang and Qing He contributed equally to this work. This work was jointly supported by the National Natural Science Foundation of China (42030612, 41888101, 41521004, 41975010, 41875023, 41875019, 41775030, and 41905009), the second Tibetan Plateau Scientific Expedition and Research Program (2019QZKK010206 and 2019QZKK0602), the Tianshan Youth Talents Plan Project of Xinjiang (2019Q038), the Strategic Priority Research Program of Chinese Academy of Sciences (XDA20100306), the Flexible Talents Introducing Project of Xinjiang (2018), and the National Department of Public Benefit (Meteorology) Research Foundation (GYHY201306066). Also, the observation instruments of DECON are continuously supported by the Repair and Purchase Projects of the Ministry of Finance of China.

References

- Chen, S., J. Huang, Y. Qian, J. Ge, and J. Su, 2014: Effects of aerosols on autumn precipitation over mid-eastern China. *J. Trop. Meteor.*, **20**, 242–250.
- , and Coauthors, 2017a: Emission, transport and radiative effects of mineral dust from Taklimakan and Gobi Deserts: Comparison of measurements and model results. *Atmos. Chem. Phys.*, **17**, 2401–2421, <https://doi.org/10.5194/acp-17-2401-2017>.
- , J. Huang, J. Li, R. Jia, N. Jiang, L. Kang, X. Ma, and T. Xie, 2017b: Comparison of dust emissions, transport, and deposition between the Taklimakan Desert and Gobi Desert from 2007 to 2011. *Sci. China Earth Sci.*, **60**, 1338–1355, <https://doi.org/10.1007/s11430-016-9051-0>.
- Eguchi, K., I. Uno, K. Yumimoto, T. Takemura, A. Shimizu, N. Sugimoto, and Z. Liu, 2009: Trans-Pacific dust transport: Integrated analysis of NASA/CALIPSO and a global aerosol transport model. *Atmos. Chem. Phys.*, **9**, 3137–3145, <https://doi.org/10.5194/acp-9-3137-2009>.
- Fa, K., Y. Zhang, B. Wu, S. Qin, Z. Liu, and W. She, 2016: Patterns and possible mechanisms of soil CO₂ uptake in sandy soil. *Sci. Total Environ.*, **544**, 587–594, <https://doi.org/10.1016/j.scitotenv.2015.11.163>.
- Filonchik, M., V. Hurnovich, H. Yan, and S. Yang, 2020: Atmospheric pollution assessment near potential source of natural aerosols in the south Gobi Desert region, China. *GISci. Remote Sens.*, **57**, 227–244, <https://doi.org/10.1080/15481603.2020.1715591>.
- Ge, J., J. Huang, C. Xu, Y. Qi, and H. Liu, 2014: Characteristics of Taklimakan dust emission and distribution: A satellite and reanalysis field perspective. *J. Geophys. Res. Atmos.*, **119**, 11 772–11 783, <https://doi.org/10.1002/2014JD022280>.
- Gong, S., X. Zhang, T. Zhao, I. G. McKendry, D. A. Jaffe, and N. Lu, 2003: Characterization of soil dust aerosol in China and its transport and distribution during 2001 ACE-Asia: 2. Model simulation and validation. *J. Geophys. Res.*, **108**, 4262, <https://doi.org/10.1029/2002JD002633>.
- Han, W., L. Yu, Z. Lai, D. Madsen, and S. Yang, 2014: The earliest well-dated archaeological site in the hyper-arid Tarim basin and its implications for prehistoric human migration and climatic change. *Quat. Res.*, **82**, 66–72, <https://doi.org/10.1016/j.yqres.2014.02.004>.
- Han, Y., X. Fang, L. Song, Q. Zhang, and S. Yang, 2005: A study of atmospheric circulation and dust storm causes of formation in the Tarim basin—The restructured wind field by shapes of dune and observed prevailing wind (in Chinese). *Chin. J. Atmos. Sci.*, **29**, 627–635.
- Hastings, S. J., W. C. Oechel, and A. Muhlia-Melo, 2005: Diurnal, seasonal and annual variation in the net ecosystem CO₂ exchange of a desert shrub community (sarcocaulis) in Baja California, Mexico. *Global Change Biol.*, **11**, 927–939, <https://doi.org/10.1111/j.1365-2486.2005.00951.x>.
- Huang, J., and Coauthors, 2007: Summer dust aerosols detected from CALIPSO over the Tibetan Plateau. *Geophys. Res. Lett.*, **34**, L18805, <https://doi.org/10.1029/2007GL029938>.
- , P. Minnis, B. Chen, Z. Huang, Z. Liu, Q. Zhao, H. Yi, and J. K. Ayers, 2008: Long-range transport and vertical structure of Asian dust from CALIPSO and surface measurements during PACDEX. *J. Geophys. Res.*, **113**, D23212, <https://doi.org/10.1029/2008JD010620>.
- , T. Wang, W. Wang, Z. Li, and H. Yan, 2014: Climate effects of dust aerosols over East Asian arid and semiarid regions. *J. Geophys. Res. Atmos.*, **119**, 11 398–11 416, <https://doi.org/10.1002/2014JD021796>.
- , and Coauthors, 2017: Dryland climate change recent progress and challenges. *Rev. Geophys.*, **55**, 719–778, <https://doi.org/10.1002/2016RG000550>.
- Huang, Y., Q. Yan, and C. Zhang, 2018: Spatial–temporal distribution characteristics of PM_{2.5} in China in 2016. *J. Geovisualization Spat. Anal.*, **2**, 12, <https://doi.org/10.1007/s41651-018-0019-5>.
- Huo, W., Q. He, X. Yang, X. Liu, G. Ding, and Y. Cheng, 2011: The research on grain size characteristic of desert in north of China (in Chinese). *Res. Soil Water Conserv.*, **18**, 6–11.
- Li, H., X. Wu, M. Ali, W. Huo, X. Yang, F. Yang, Q. He, and Y. Liu, 2016: Estimating surface broadband emissivity of the Taklimakan Desert with FTIR and MODIS data (in Chinese). *Guangpuxue Yu Guangpu Fenxi*, **36**, 2414–2419.
- Li, Y., Y. Wang, R. A. Houghton, and L. Tang, 2015: Hidden carbon sink beneath desert. *Geophys. Res. Lett.*, **42**, 5880–5887, <https://doi.org/10.1002/2015GL064222>.
- Liu, C., 2016: Observation, parameterization and climate simulation of dust emission processes (in Chinese). M.S. thesis, School of Atmospheric Physics, Nanjing University of Information Science and Technology, 51 pp.
- Liu, J., Y. Zheng, Z. Li, C. Flynn, E. J. Welton, and M. Cribb, 2011: Transport, vertical structure and radiative properties of dust events in southeast China determined from ground and space sensors. *Atmos. Environ.*, **45**, 6469–6480, <https://doi.org/10.1016/j.atmosenv.2011.04.031>.
- Liu, X., L. Li, and Z. An, 2001: Tibetan Plateau uplift and drying in Eurasian interior and Northern Africa (in Chinese). *Quat. Sci.*, **21**, 114–122.
- Liu, Y., Q. He, H. Zhang, and M. Ali, 2012: Improving the CoLM in Taklimakan Desert hinterland with accurate key parameters and an appropriate parameterization scheme. *Adv. Atmos. Sci.*, **29**, 381–390, <https://doi.org/10.1007/s00376-011-1068-6>.
- Liu, Y., Q. Zhu, J. Huang, S. Hua, and R. Jia, 2019: Impact of dust-polluted convective clouds over the Tibetan Plateau on downstream precipitation. *Atmos. Environ.*, **209**, 67–77, <https://doi.org/10.1016/j.atmosenv.2019.04.001>.
- , Y. Li, J. Huang, Q. Zhu, and S. Wang, 2020a: Attribution of the Tibetan Plateau to northern drought. *Natl. Sci. Rev.*, **7**, 489–492, <https://doi.org/10.1093/nsr/nwz191>.
- , Q. Zhu, S. Hua, K. Alam, T. Dai, and Y. Cheng, 2020b: Tibetan Plateau driven impact of Taklimakan dust on northern rainfall. *Atmos. Environ.*, **234**, 117583, <https://doi.org/10.1016/j.atmosenv.2020.117583>.
- Ma, J., Z. Wang, B. A. Stevenson, X. Zheng, and Y. Li, 2013: An inorganic CO₂ diffusion and dissolution process explains negative CO₂ fluxes in saline/alkaline soils. *Sci. Rep.*, **3**, 2025, <https://doi.org/10.1038/srep02025>.
- , R. Liu, L. Tang, Z. Lan, and Y. Li, 2014: A downward CO₂ flux seems to have nowhere to go. *Biogeosciences*, **11**, 6251–6262, <https://doi.org/10.5194/bg-11-6251-2014>.
- Ma, Y., S. Kang, L. Zhu, B. Xu, L. Tian, and T. Yao, 2008: Tibetan Observation and Research Platform: Atmosphere–land interaction over a heterogeneous landscape. *Bull. Amer. Meteor. Soc.*, **89**, 1487–1492.
- , and Coauthors, 2017: Monitoring and modeling the Tibetan Plateau's climate system and its impact on East Asia. *Sci. Rep.*, **7**, 44574, <https://doi.org/10.1038/srep44574>.
- , and Coauthors, 2020: A long-term (2005–2016) dataset of hourly integrated land–atmosphere interaction observations on the Tibetan Plateau. *Earth Syst. Sci. Data*, **12**, 2937–2957, <https://doi.org/10.5194/essd-12-2937-2020>.
- Manabe, S., and A. J. Broccoli, 1990: Mountains and arid climates of middle latitudes. *Science*, **247**, 192–195, <https://doi.org/10.1126/science.247.4939.192>.
- Marshall, J. H., D. J. Parker, C. M. Grams, B. T. Johnson, W. Grey, and A. N. Ross, 2008: Observations of mesoscale and boundary-layer scale circulations affecting dust transport and uplift over the Sahara. *Atmos. Chem. Phys.*, **8**, 6979–6993, <https://doi.org/10.5194/acp-8-6979-2008>.
- Meng, L., and Coauthors, 2019: Modeling study on three-dimensional distribution of dust aerosols during a dust storm over the Tarim basin, northwest China. *Atmos. Res.*, **218**, 285–295, <https://doi.org/10.1016/j.atmosres.2018.12.006>.
- Shao, Y., and Coauthors, 2011: Dust cycle: An emerging core theme in Earth system science. *Aeolian Res.*, **2**, 181–204, <https://doi.org/10.1016/j.aeolia.2011.02.001>.
- Stone, R., 2008: Have desert researchers discovered a hidden loop in the carbon cycle? *Science*, **320**, 1409–1410, <https://doi.org/10.1126/science.320.5882.1409>.
- Wang, M., H. Ming, W. Huo, H. Xu, J. Li, and X. Li, 2017: Detecting sand-dust storms using a wind-profiling radar. *J. Arid Land*, **9**, 753–762, <https://doi.org/10.1007/s40333-017-0031-5>.
- , ——, Z. Ruan, L. Gao, and D. Yang, 2018: Quantitative detection of mass concentration of sand-dust storms via wind-profiling radar and analysis of Z-M relationship. *Theor. Appl. Climatol.*, **131**, 927–935, <https://doi.org/10.1007/s00704-016-2012-6>.

- Wang, S., J. Wang, Z. Zhou, and K. Shang, 2005: Regional characteristics of three kinds of dust storm events in China. *Atmos. Environ.*, **39**, 509–520, <https://doi.org/10.1016/j.atmosenv.2004.09.033>.
- Wang, Y., and Coauthors, 2016: Analysis of land surface parameters and turbulence characteristics over the Tibetan Plateau and surrounding region. *J. Geophys. Res. Atmos.*, **121**, 9540–9560, <https://doi.org/10.1002/2016JD025401>.
- Wohlfahrt, G., L. Fenstermaker, and J. Arnone, 2008: Large annual net ecosystem CO₂ uptake of a Mojave Desert ecosystem. *Global Change Biol.*, **14**, 1475–1487, <https://doi.org/10.1111/j.1365-2486.2008.01593.x>.
- Xinjiang Bureau of Statistics, 2017: *Xinjiang Statistical Yearbook 2016* (in Chinese). China Statistics Press, 21 pp.
- Xu, X., T. Zhao, C. Lu, and X. Shi, 2014: Characteristics of the water cycle in the atmosphere over the Tibetan Plateau (in Chinese). *Acta Meteor. Sin.*, **72**, 1079–1095.
- Yang, F., X. Yang, W. Huo, M. Ali, X. Zheng, C. Zhou, and Q. He, 2017a: A continuously weighing, high frequency sand trap: Wind tunnel and field evaluations. *Geomorphology*, **293**, 84–92, <https://doi.org/10.1016/j.geomorph.2017.04.008>.
- , M. Ali, X. Zheng, Q. He, X. Yang, W. Huo, F. Liang, and S. Wang, 2017b: Diurnal dynamics of soil respiration and the influencing factors for three land-cover types in the hinterland of the Taklimakan Desert, China. *J. Arid Land*, **9**, 568–579, <https://doi.org/10.1007/s40333-017-0060-0>.
- , and Coauthors, 2020a: Taklimakan desert carbon-sink decreases under climate change. *Sci. Bull.*, **65**, 431–433, <https://doi.org/10.1016/j.scib.2019.12.022>.
- , and Coauthors, 2020b: Impact of differences in soil temperature on the desert carbon sink. *Geoderma*, **379**, 114636, <https://doi.org/10.1016/j.geoderma.2020.114636>.
- Yang, K., and Coauthors, 2007: Initial CEOP-based review of the prediction skill of operational general circulation models and land surface models. *J. Meteor. Soc. Japan*, **85A**, 99–116, <https://doi.org/10.2151/jmsj.85A.99>.
- Yang, X., 2019: Observation and parameterization on dust emission over the Taklimakan Desert (in Chinese). Ph.D. thesis, School of Applied Meteorology, Nanjing University of Information Science and Technology, 77 pp.
- , S. Shen, F. Yang, Q. He, M. Ali, W. Huo, and X. Liu, 2016a: Spatial and temporal variations of blowing dust events in the Taklimakan Desert. *Theor. Appl. Climatol.*, **125**, 669–677, <https://doi.org/10.1007/s00704-015-1537-4>.
- , F. Yang, X. Liu, W. Huo, M. Ali, and Q. Zhang, 2016b: Comparison of horizontal dust fluxes simulated with two dust emission schemes based on field experiments in Xinjiang, China. *Theor. Appl. Climatol.*, **126**, 223–231, <https://doi.org/10.1007/s00704-015-1573-0>.
- , —, C. Zhou, M. Alia, W. Huo, and Q. He, 2020: Improved parameterization for effect of soil moisture on threshold friction velocity for saltation activity based on observations in the Taklimakan Desert. *Geoderma*, **369**, 114322, <https://doi.org/10.1016/j.geoderma.2020.114322>.
- Ye, D., and Y. Gao, 1979: *The Meteorology of Qinghai-Xizang Plateau* (in Chinese). Science Press, 278 pp.
- Zhang, Q., and S. Wang, 2008: A study on atmospheric boundary layer structure on a clear day in the arid region in northwest China (in Chinese). *Acta Meteor. Sin.*, **66**, 599–608.
- Zhang, X., S. Gong, T. Zhao, R. Arimoto, Y. Wang, and Z. Zhou, 2003: Sources of Asian dust and role of climate change versus desertification in Asian dust emission. *Geophys. Res. Lett.*, **30**, 2272, <https://doi.org/10.1029/2003GL018206>.